Supporting Information

Seawater-Assisted Biomass Upgrading with Stable Catalytic Activity for 1500 hours

Yujie Ren[a, b, 1], Bin Zhu[a, 1], Qiuge Wang[a, c], Shuyi Wang[d], Sheng Chen[a], Jian Zhang[a, c, *], Chunlin Chen[a, c, *]

[a] *Key Laboratory of Biobased Polymeric Materials of Zhejiang Province, Ningbo Institute of Materials Technology & Engineering, Chinese Academy of Sciences, 1219 Zhongguan West Road, Ningbo 315201, China.*
[b] *Zhejiang University of Technology, College of Materials Science and Engineering, Hangzhou 310014, China.*
[c] *University of Chinese Academy of Sciences, Beijing 100049, China.*
[d] *North China University of Science and Technology, College of Chemical Engineering, Tangshan, 063210, China.*

[1] These authors contributed equally to this work.

[*] Corresponding author.

E-mail address: jzhang@nimte.ac.cn (J. Zhang); chenchunlin@nimte.ac.cn (C. Chen)

Table S1. The corrosion layer loading of NF-sw-120.

Number	$m_{cleaned}$ (g)	$m_{NF\text{-}sw\text{-}120}$ (g)	$m_{corrosion}$ (g)	Average loading amount
1	0.0456	0.0510	0.0054	
2	0.0481	0.0528	0.0047	
3	0.0491	0.0555	0.0064	8.77 wt%
4	0.0444	0.0474	0.0030	
5	0.0447	0.0478	0.0031	

Table S2. Product analysis results of NF-DI-120 electrolysis of 10 mM HMF at constant potential of 1.45 V vs. RHE.

	Conversion	FDCA Yield	FE	Carbon balance
Percentage (%)	99.5	78.5	80.2	82.3

Table S3. The comparison of the HMFOR ability of NF-sw-120 in this work with recently reported electrocatalysts.

Catalysts	Electrolytic potential (V vs. RHE)	HMF concentration (mM)	Conversion (%)	FDCA Yield (%)	FE (%)	References
$NiFePBA/Ni(OH)_2$	1.47	10	99.1	97.6	94.2	[1]
NiFe-ZIF/S-900	1.50	10	100	96.2	96.0	[2]
NCSP150	1.52	10	99.0	92.5	95.2	[3]
Co_3O_4-NiO	1.22	10	97.0	83.3	89.5	[4]
NCO-0.75	1.50	10	100	96.0	93.8	[5]
Ni_2Co_1-MOF	1.35	5	100	97.3	90.0	[6]
$Ni_{0.5}Co_{2.5}O_4$	1.50	10	100	92.4	90.3	[7]
$NiMoO_4$-CNTs-CF	1.35	10	96.3	93.8	89.4	[8]
FeCoNi-S@NF	1.45	10	95.7	94.8	94.7	[9]
Co_3O_4/NF	1.43	10	100	96.7	96.5	[10]
NF-sw-120	1.45	10	100	98.3	95.8	This Work
NF-sw-120 (seawater)	1.45	10	100	97.5	97.6	This Work

Table S4. Results of the analysis of the product produced by electrolysis of 10 mM HMF at a constant potential of 1.45 V vs. RHE for the NF-sw-120 electrode after continuous operation in alkaline seawater for 1500 h.

	Conversion	FDCA Yield	FE	Carbon balance
Percentage (%)	100	96.8	95.2	98.8

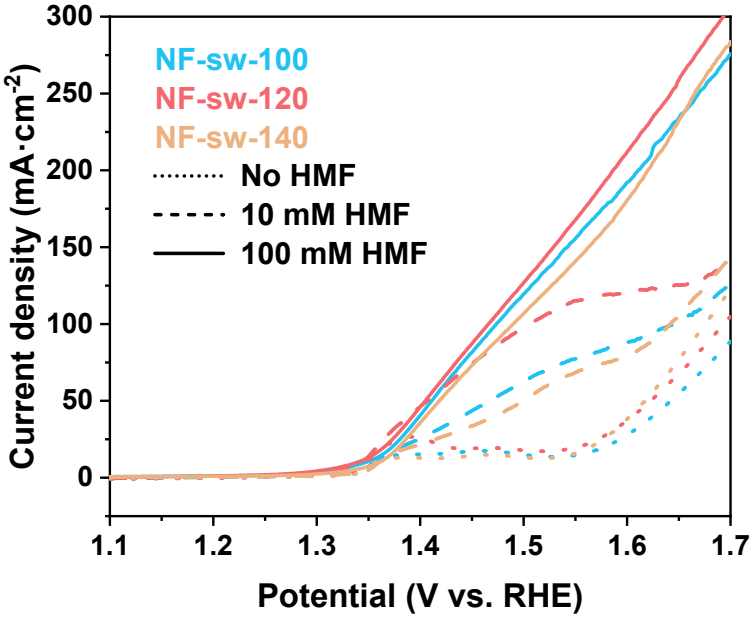

Figure S1. LSV curves of the NF-sw-T in 1 M KOH electrolyte with different HMF concentrations.

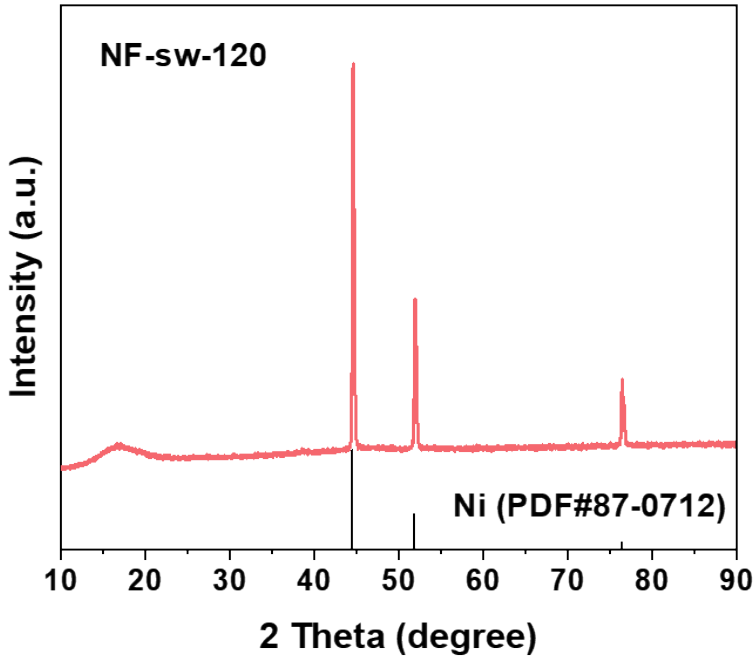

Figure S2. XRD spectra of NF-sw-120.

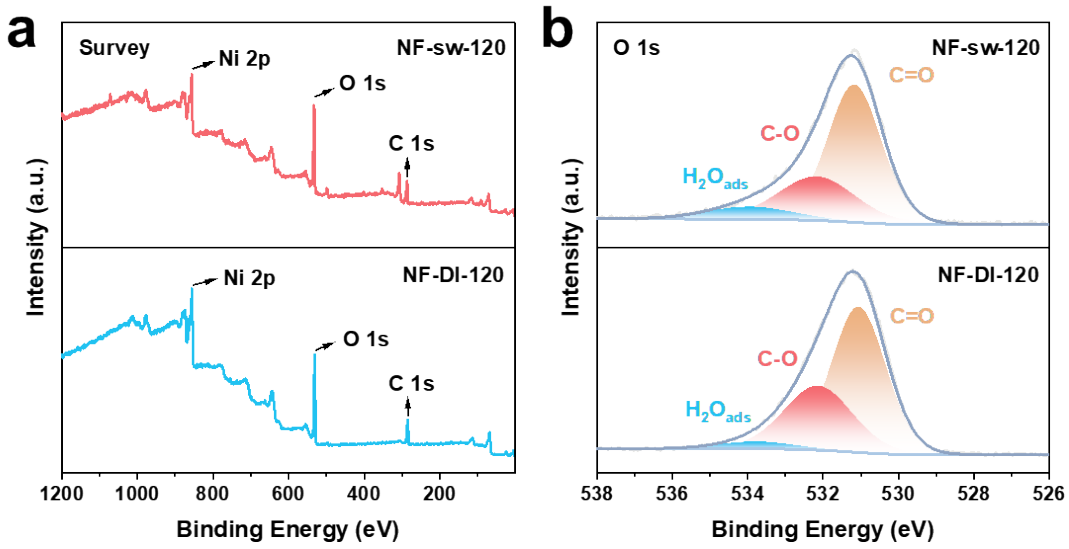

Figure S3. The XPS spectra of (a) survey, (b) O 1s of NF-sw-120 and NF-DI-120.

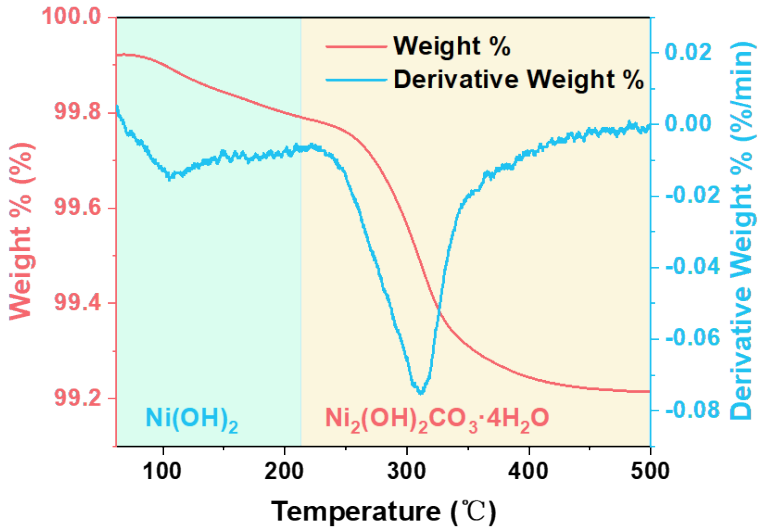

Figure S4. TG and its derivative curves of NF-sw-120.

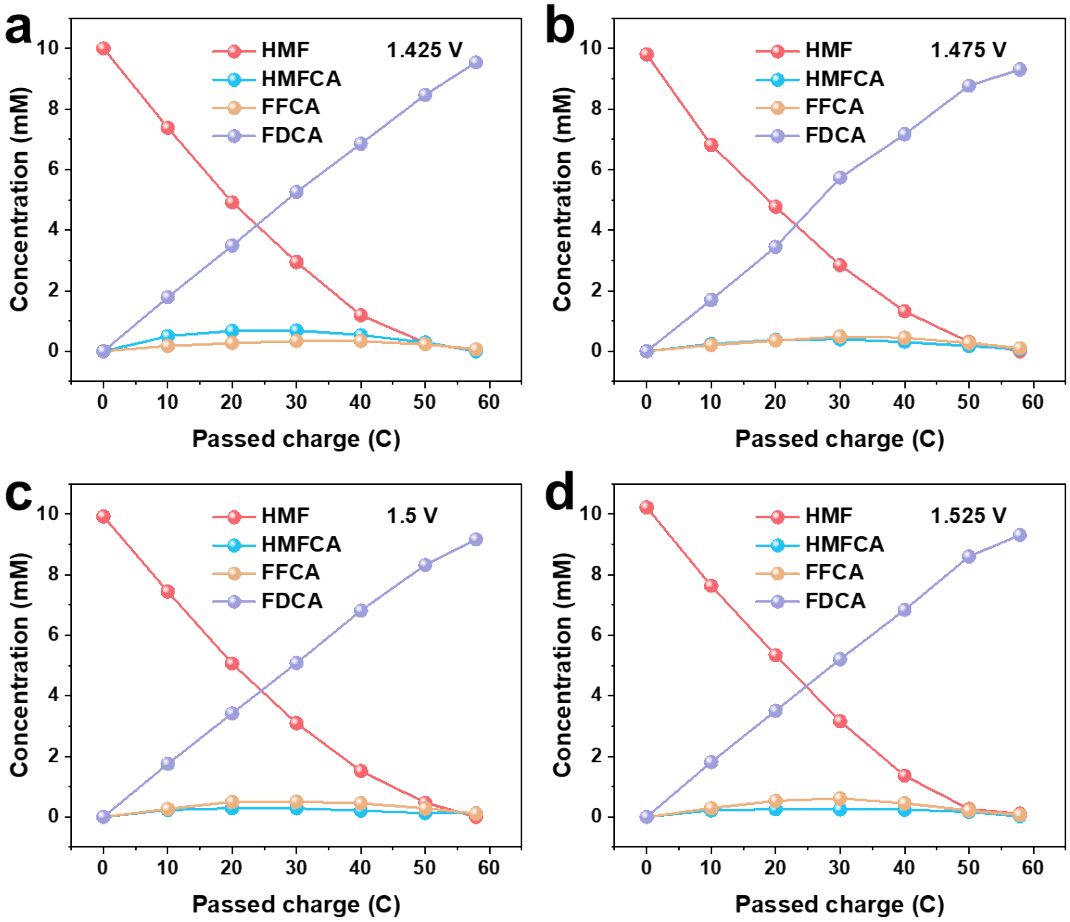

Figure S5. The time-course profile of NF-sw-120 at different electrolysis potentials.

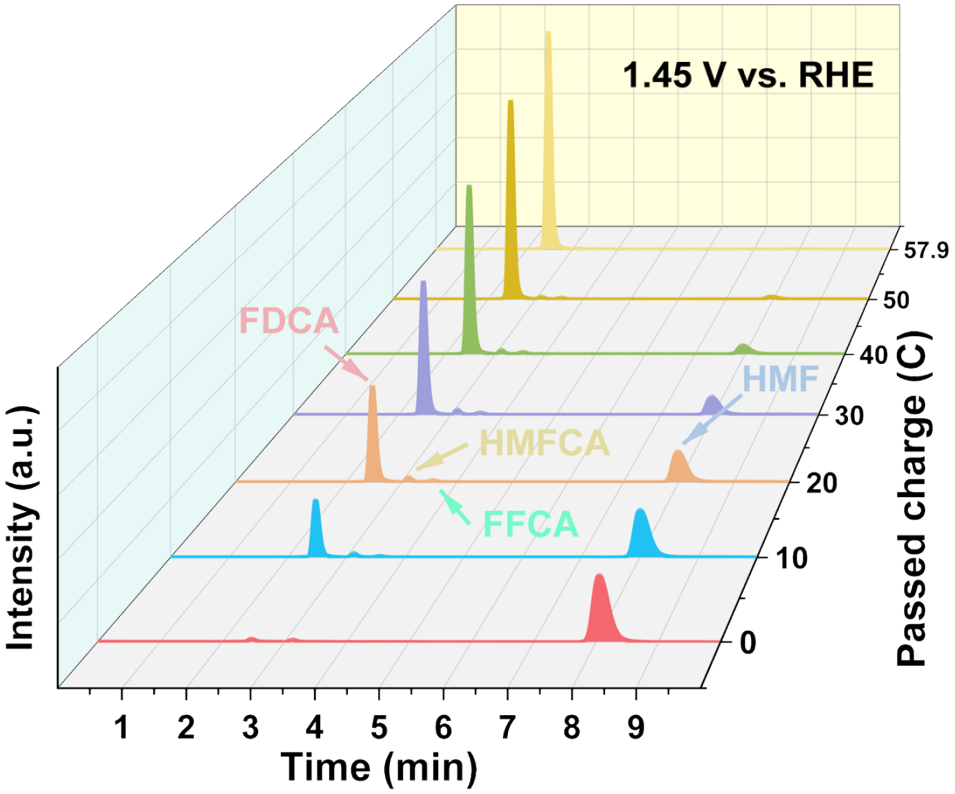

Figure S6. The corresponding HPLC curves at different charges.

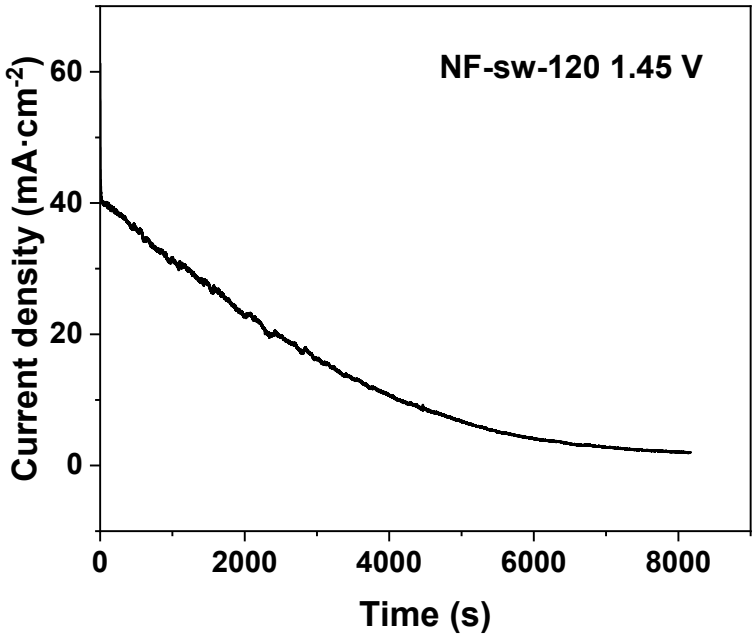

Figure S7. The chronoamperometric curve of the NF-sw-120 electrode at a potential of 1.45 V.

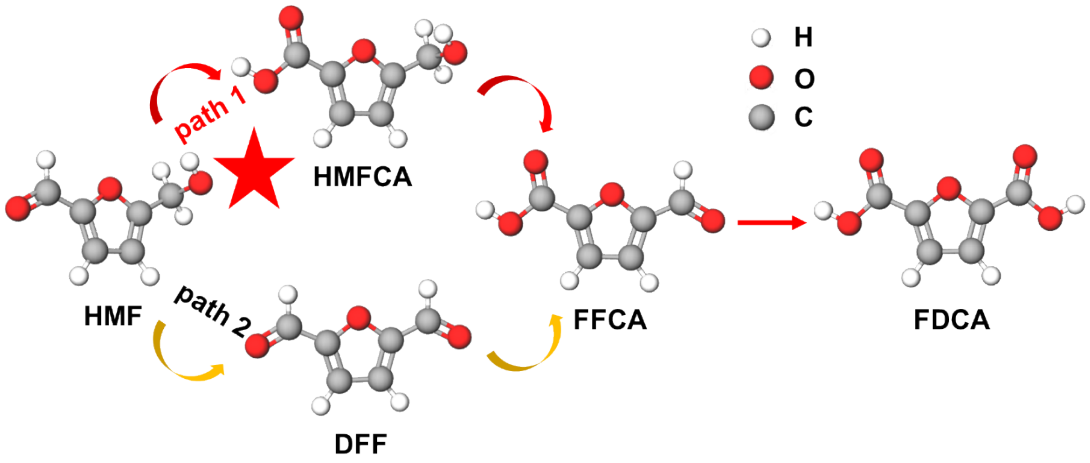

Figure S8. Reaction routes for HMF oxidation to FDCA.

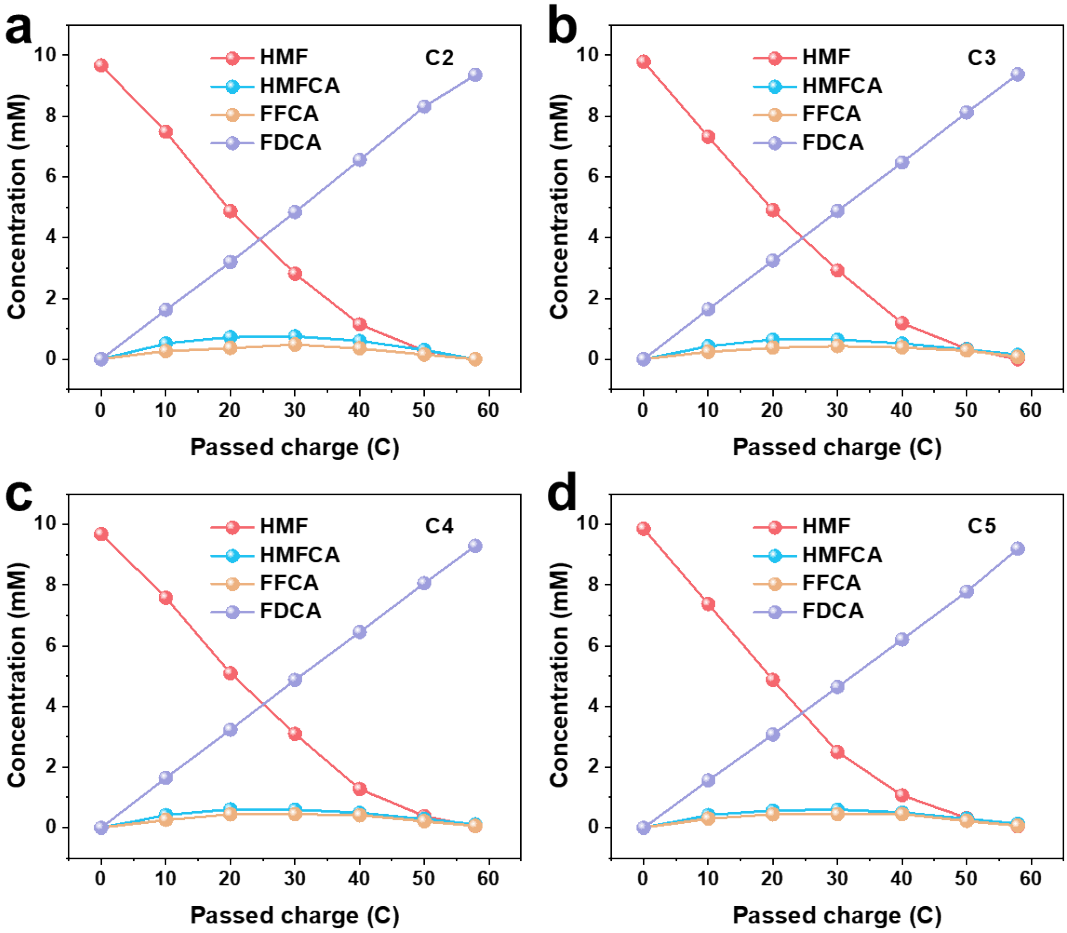

Figure S9. The time-course profile of NF-sw-120 under cyclic electrolysis tests.

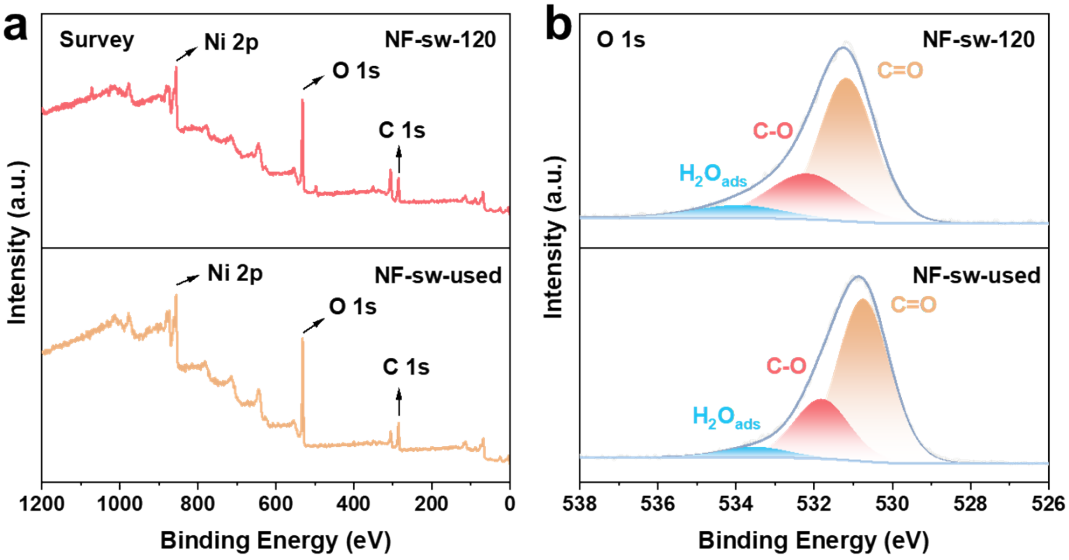

Figure S10. The XPS spectra of (a) survey, (b) O 1s of NF-sw-120 before and after use.

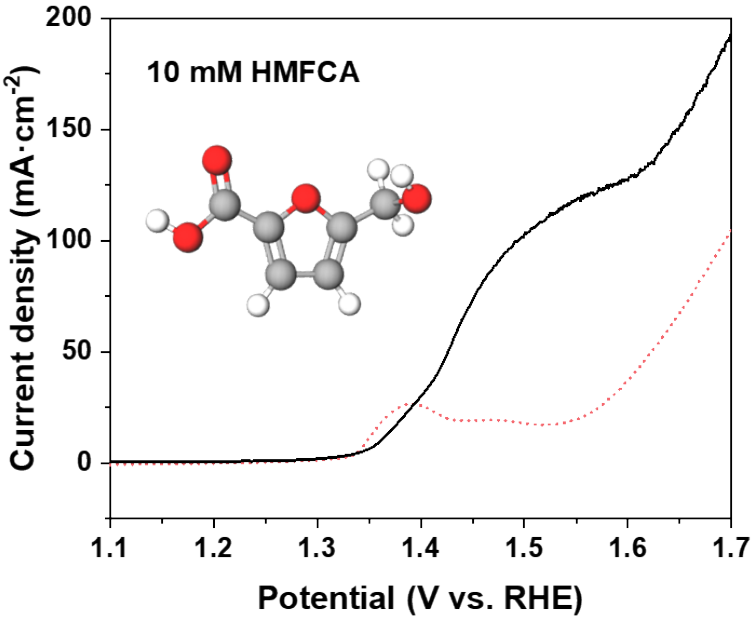

Figure S11. LSV curves of the NF-sw-120 in 1 M KOH electrolyte with HMFCA.

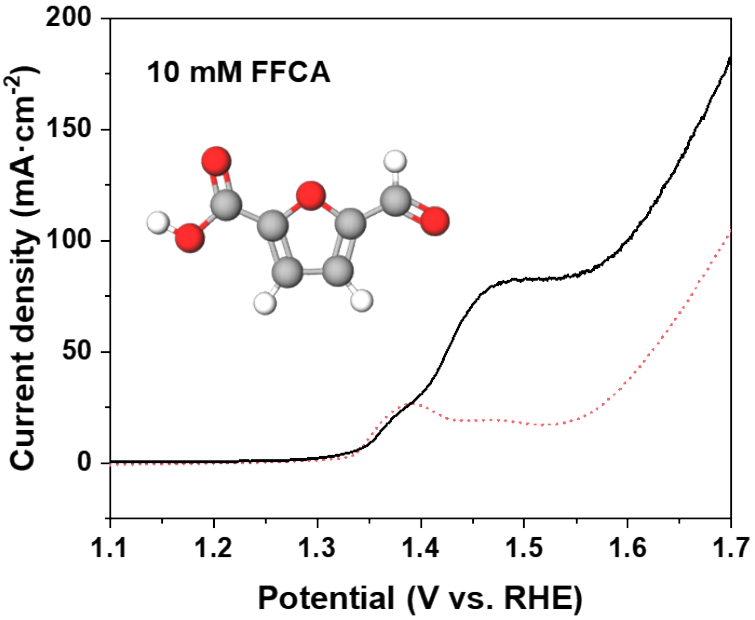

Figure S12. LSV curves of the NF-sw-120 in 1 M KOH electrolyte with FFCA.

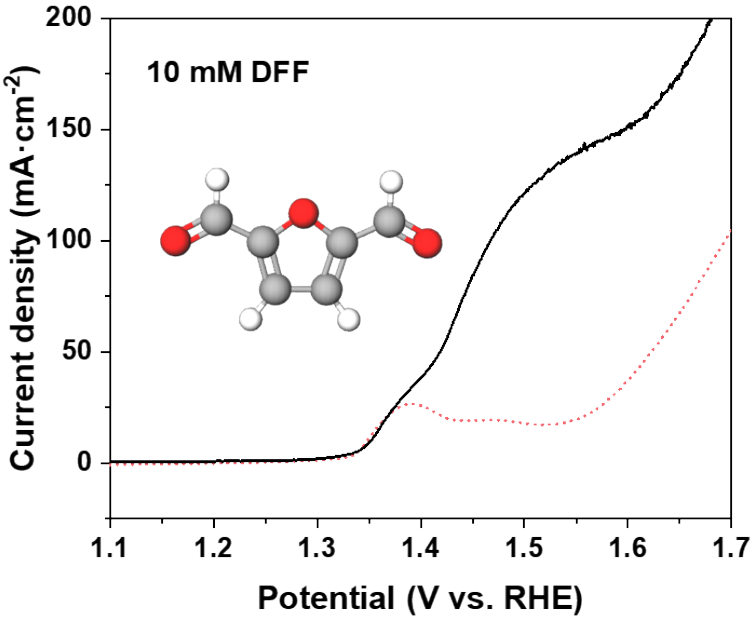

Figure S13. LSV curves of the NF-sw-120 in 1 M KOH electrolyte with DFF.

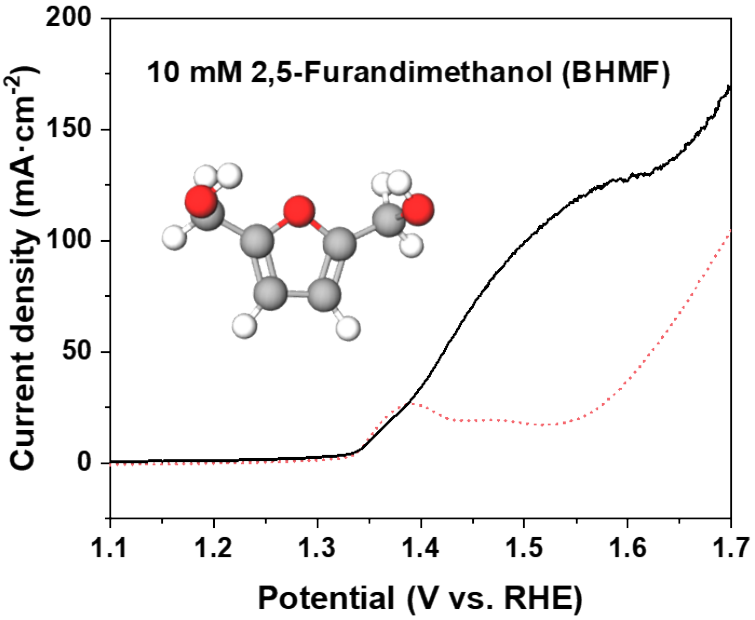

Figure S14. LSV curves of the NF-sw-120 in 1 M KOH electrolyte with BHMF.

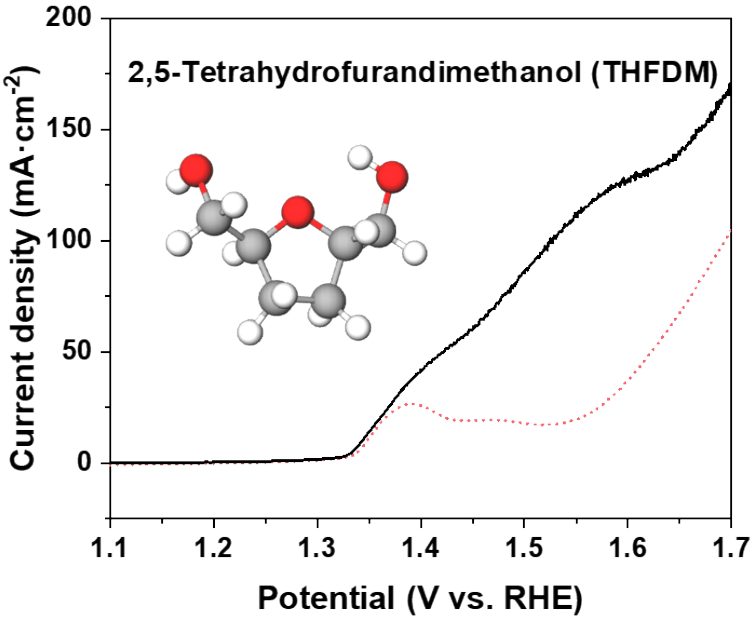

Figure S15. LSV curves of the NF-sw-120 in 1 M KOH electrolyte with 2,5-tetrahydrofurandimethanol.

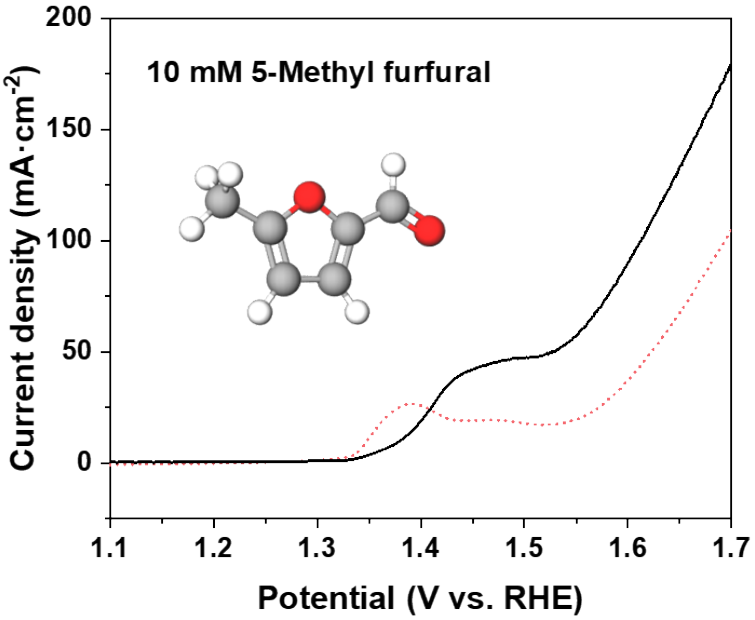

Figure S16. LSV curves of the NF-sw-120 in 1 M KOH electrolyte with 5-methyl furfural.

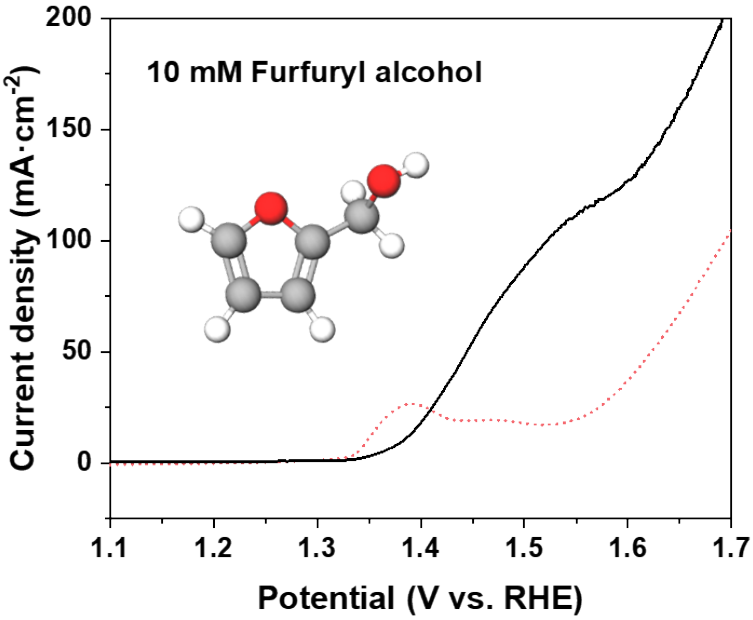

Figure S17. LSV curves of the NF-sw-120 in 1 M KOH electrolyte with furfuryl alcohol.

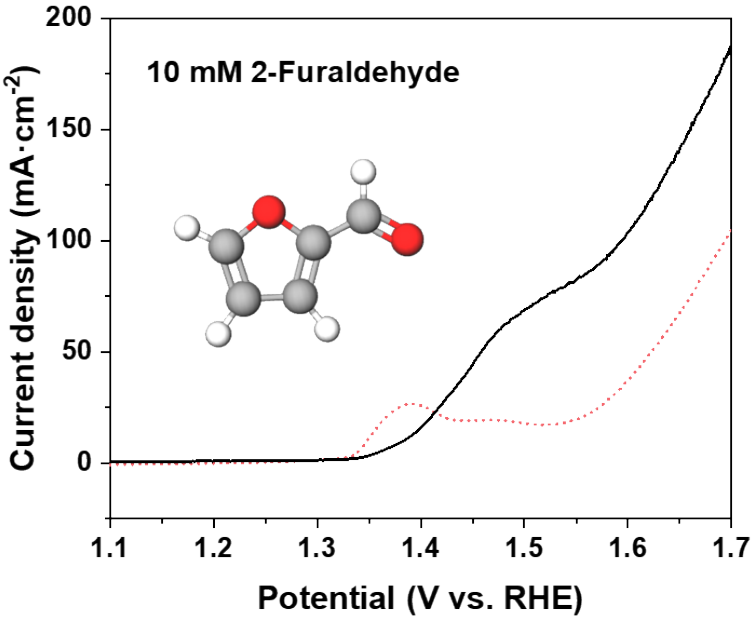

Figure S18. LSV curves of the NF-sw-120 in 1 M KOH electrolyte with 2-furaldehyde.

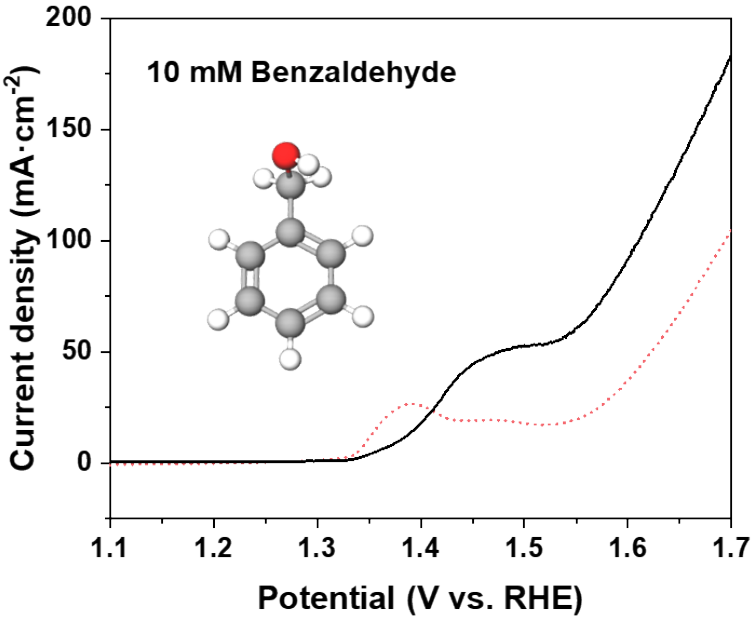

Figure S19. LSV curves of the NF-sw-120 in 1 M KOH electrolyte with benzaldehyde.

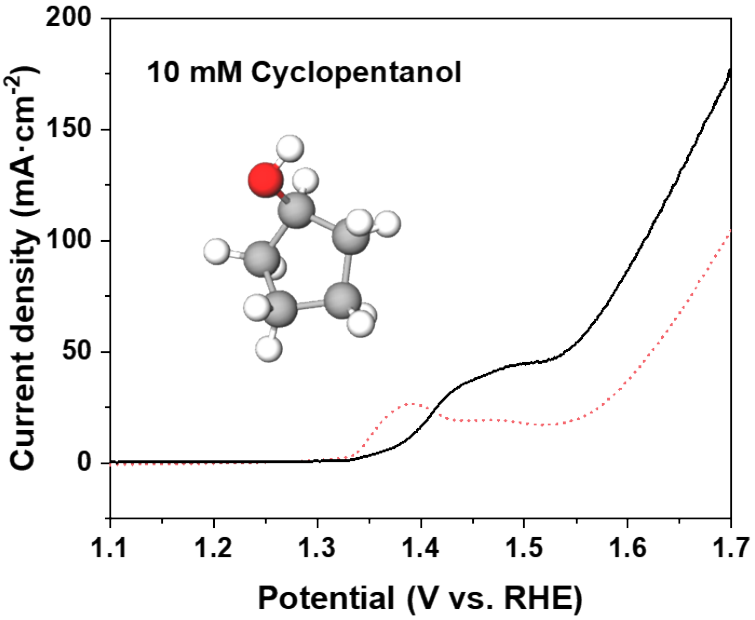

Figure S20. LSV curves of the NF-sw-120 in 1 M KOH electrolyte with cyclopentanol.

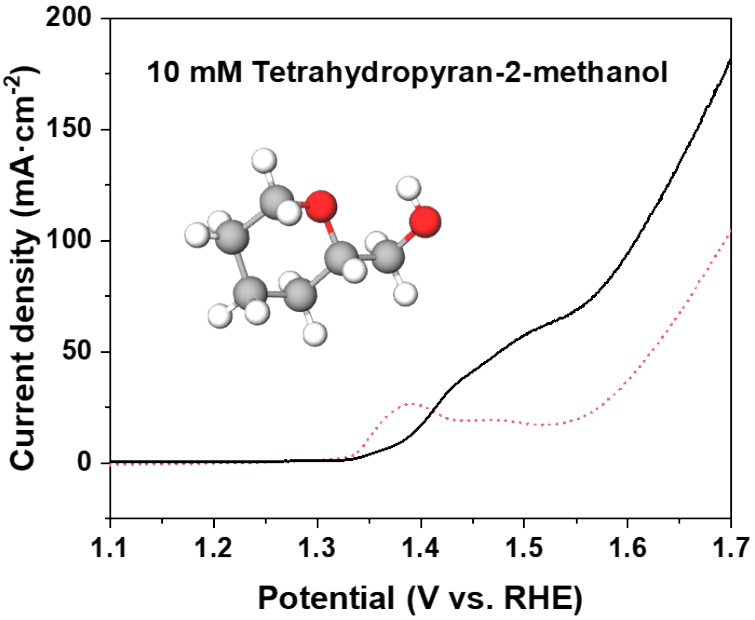

Figure S21. LSV curves of the NF-sw-120 in 1 M KOH electrolyte with tetrahydropyran-2-methanol.

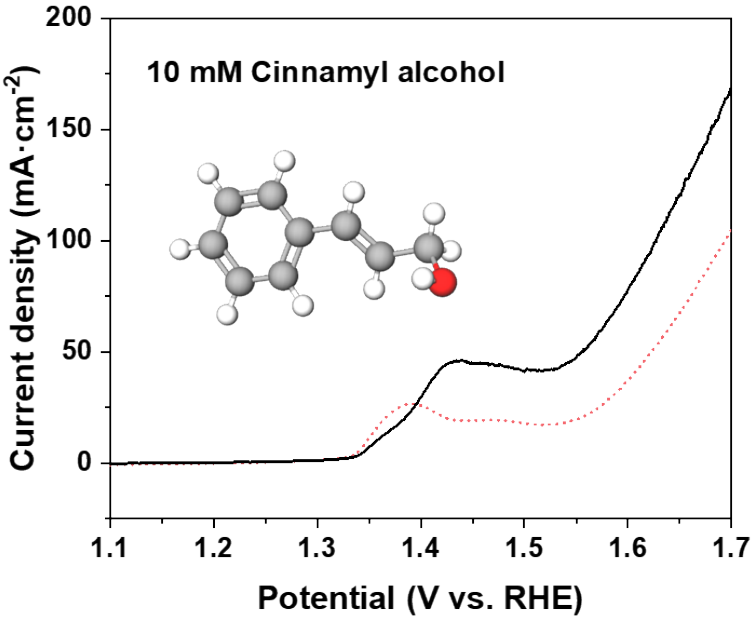

Figure S22. LSV curves of the NF-sw-120 in 1 M KOH electrolyte with cinnamyl alcohol.

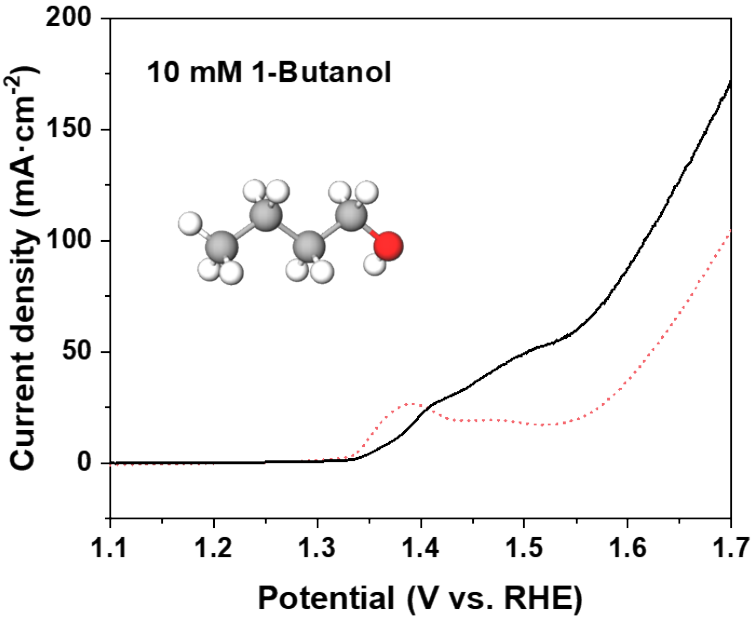

Figure S23. LSV curves of the NF-sw-120 in 1 M KOH electrolyte with 1-butanol.

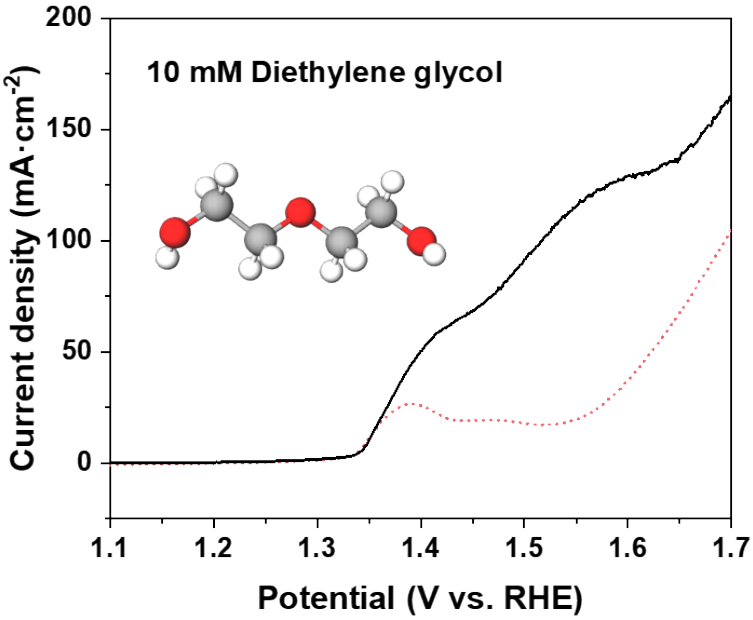

Figure S24. LSV curves of the NF-sw-120 in 1 M KOH electrolyte with diethylene glycol.

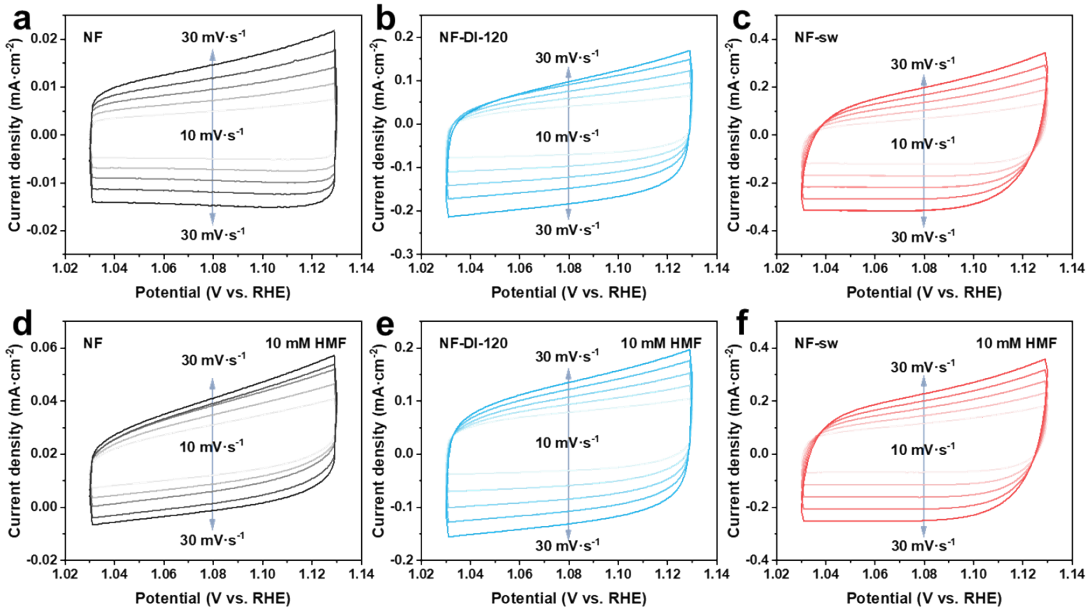

Figure S25. CV curves at different sweep speeds of NF, NF-DI-120, and NF-sw-120.

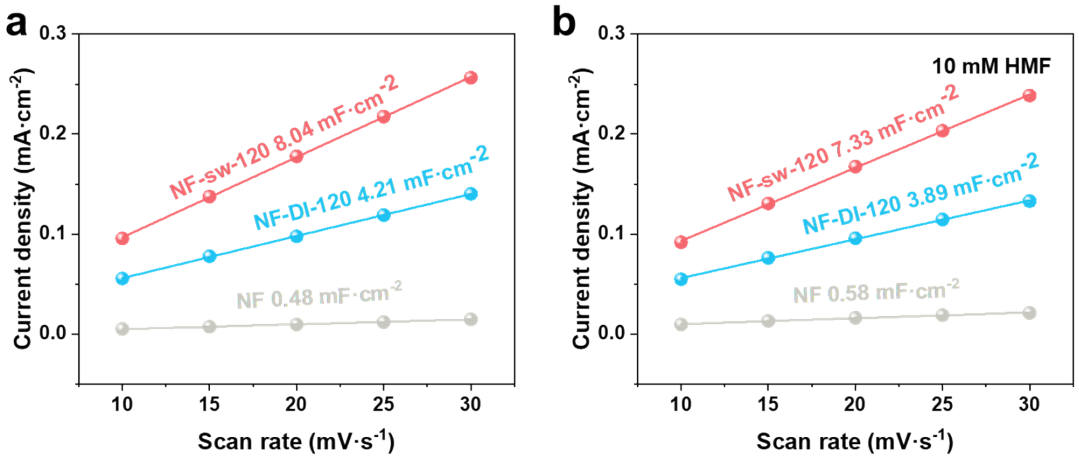

Figure S26. Double layer capacitance of NF, NF-DI-120, and NF-sw-120.

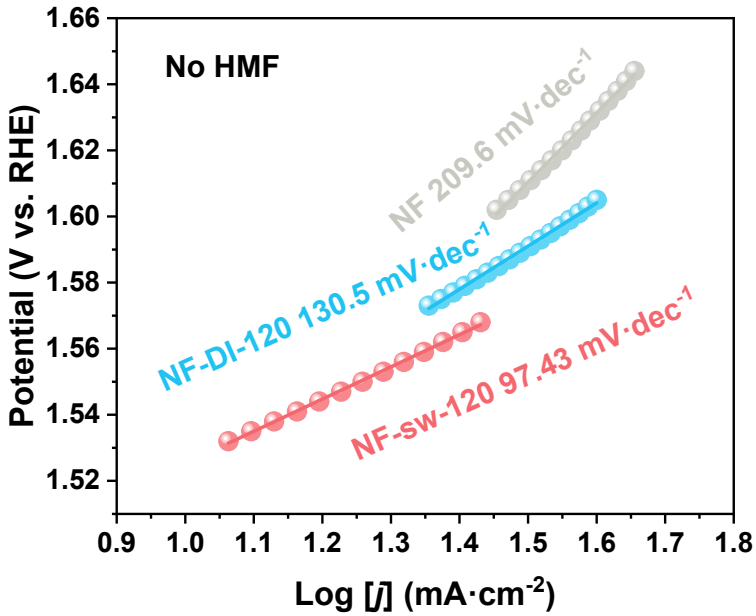

Figure S27. Tafel slope of NF-sw-120.

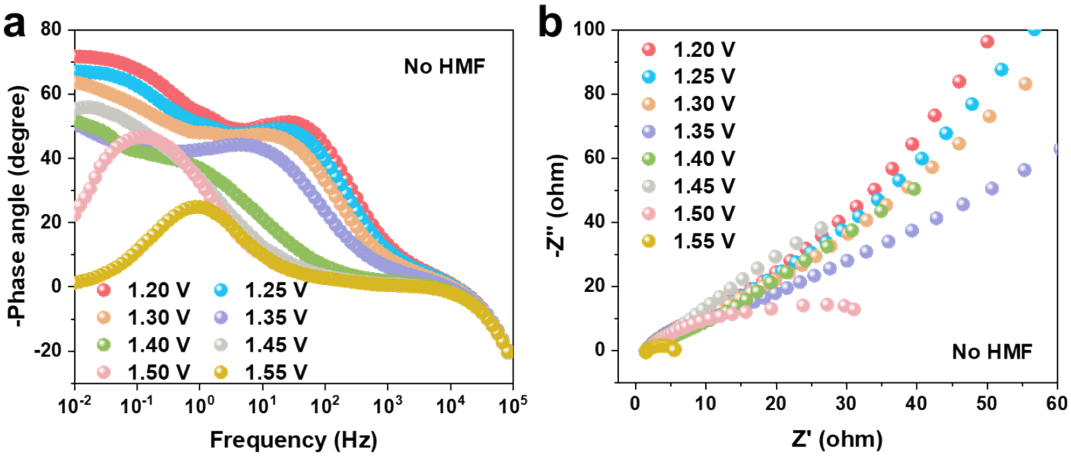

Figure S28. In situ EIS of NF-sw-120.

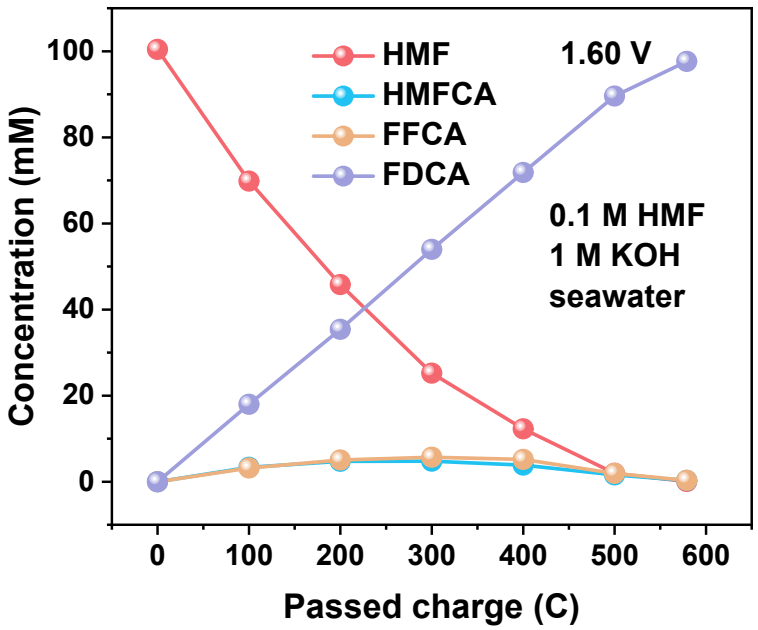

Figure S29. The time-course profile of HMFOR on NF-sw-120 at 1.60 V vs. RHE.

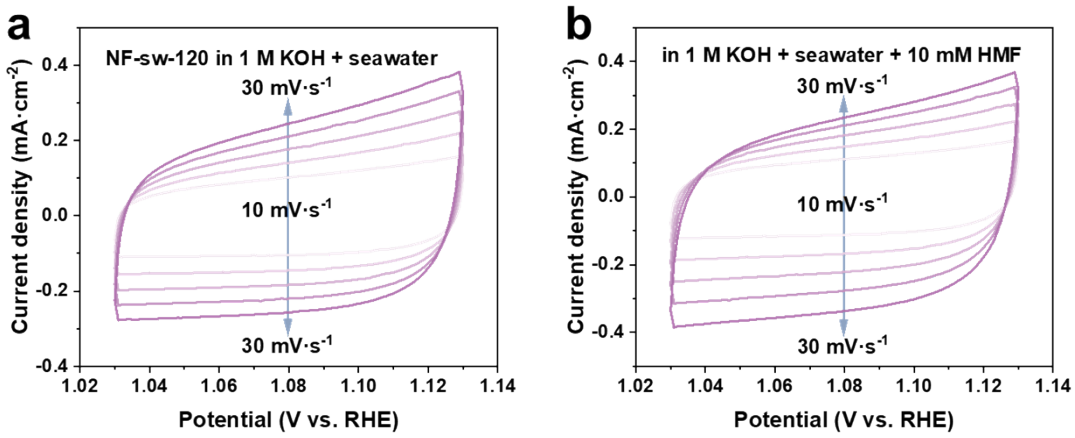

Figure S30. CV curves at different sweep speeds of NF-sw-120 (in alkaline seawater).

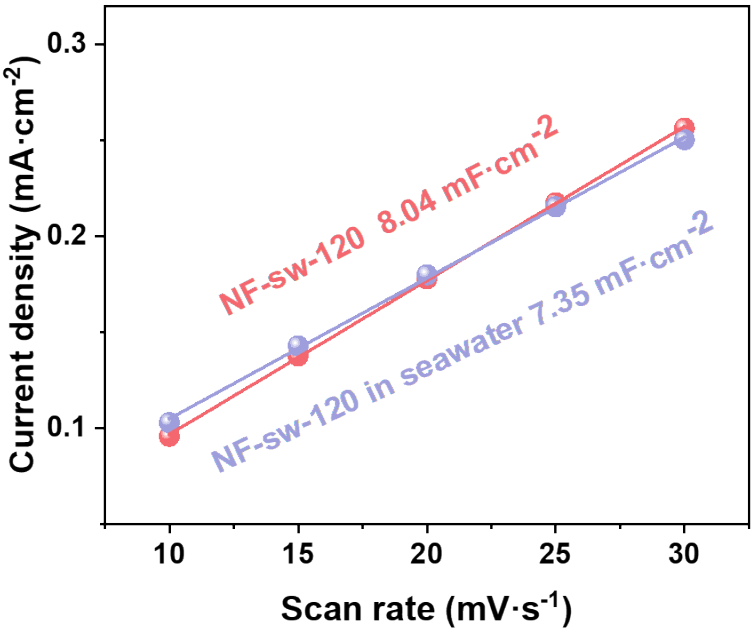

Figure S31. Double layer capacitance of NF-sw-120.

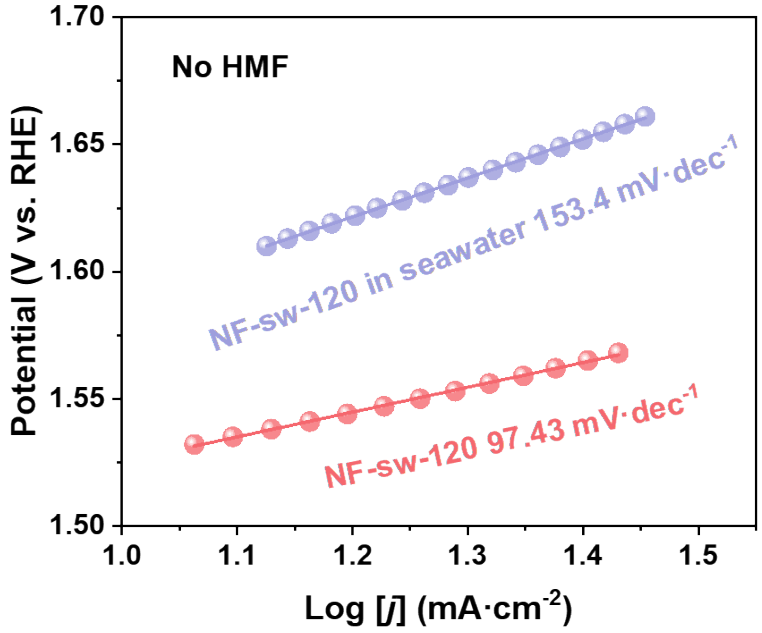

Figure S32. Tafel slope of NF-sw-120.

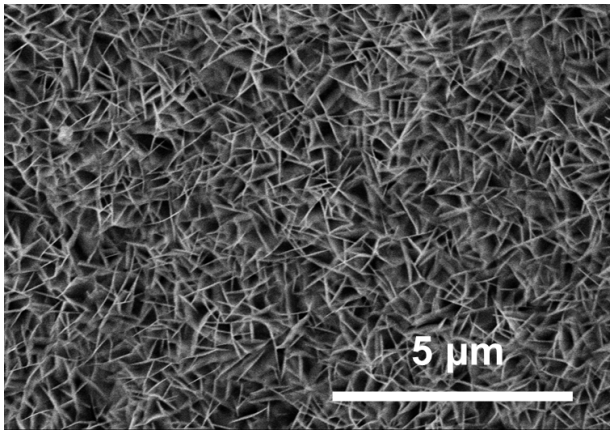

Figure S33. SEM image of the NF-sw-120 electrode used for 1500 hours.

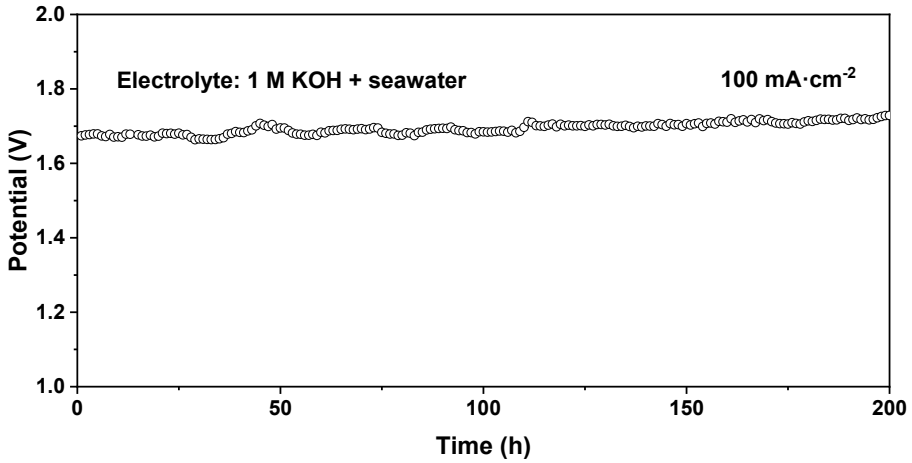

Figure S34. Stability assessment of NF-sw-120 (100 mA cm^{-2}).

References

[1] X.H. Chen, H. Liu, L. Chen, W. Xiong, Y.Q. Liu, X.J. Sun, F. Hao, An efficient catalyst from electrochemical self-reconstruction of NiFePBA/ $Ni(OH)_2$ for 5-hydroxymethylfurfural electrooxidation to produce high-valued 2,5-furandicarboxylic acid, Journal of Catalysis 447 (2025) 116159, https://doi.org/10.1016/j.jcat.2025.116159.

[2] Z.J. Yao, X. Wang, Z.H. Ma, Y. Han, Modulation of surface properties of metal organic framework-derived carbon substrates through vacancy defects for high-value biomass conversion, Journal of Colloid and Interface Science 695 (2025) 137752, https://doi.org/10.1016/j.jcis.2025.137752.

[3] K.M. Hung, J.J. Wu, Bifunctional nickel phosphide nanoparticle/nickel cobalt sulfide nanosheet framework for electrocatalytic simultaneous hydrogen evolution and 2,5-Furandicaroxylic acid production, Chemical Engineering Journal 484 (2024) 149772, https://doi.org/10.1016/j.cej.2024.149772.

[4] P.Y. Jin, L. Zhang, Z. Wu, B. Zhou, Z.J. Duan, H.Y. Li, H.W. Liu, A.M. Deng, Q.Y. Li, Y.Q. Zhang, C.X. Zhao, S.Y. Wang, Heterogeneous interface induced Co_3O_4-NiO catalyst for efficient electrocatalytic 5-Hydroxymethylfurfural oxidation, Chemical Engineering Journal 481 (2024) 148303, https://doi.org/10.1016/j.cej.2023.148303.

[5] W. Huang, X.H. Li, W. Liu, B.J. Li, Y.M. Zhou, Y.C. Wang, S.Y. Tao, Synergistic enhancement of nickel-cobalt nano-catalysts for 5-hydroxyme-thylfurfural conversion via electronic structure engineering and solar intensification, Chemical Engineering Journal 501 (2024) 157642, https://doi.org/10.1016/j.cej.2024.157642.

[6] Z.F. Zhao, M.K. Zhu, M.N. Qu, X.Y. Luo, Q.Q. Hu, X.Y. Shen, W.B. Zheng, Y. Jia, Q. Sun, J. Chen, H.J. Zheng, Relay electrocatalysis with bimetallic sites for highly efficient oxidation in multiple cascade reaction, Chemical Engineering Journal 484 (2024) 149768, https://doi.org/10.1016/j.cej.2024.149768.

[7] Y.X. Lu, T.Y. Liu, Y.C. Huang, L. Zhou, Y.Y. Li, W. Chen, L. Yang, B. Zhou, Y.D. Wu, Z.J. Kong, Z.F. Huang, Y.F. Li, C.L. Dong, S.Y. Wang, Y.Q. Zou, Integrated Catalytic Sites for Highly Efficient Electrochemical Oxidation of the Aldehyde and Hydroxyl Groups in 5-Hydroxymethylfurfural, ACS Catalysis 12 (2022) 4242-4251, https://doi.org/10.1021/acscatal.2c00174.

[8] Y. Wu, Z.L. Guo, C.X. Sun, Y.D. Yang, Q. Li, Integrated experimental and DFT analysis on the efficient and green upgrading of agroforestry biomass derived furan chemicals over $NiMoO_4$-CNTs-CF electrocatalyst with bi-catalytic sites, Industrial Crops and Products 187 (2022) 115492, https://doi.org/10.1016/j.indcrop.2022.115492.

[9] Z.Z. Lin, L.L. Wang, T.B. Jia, X. Wang, C.J. Li, H.R. Wang, L. Li, Y.T. Zhou, C.Y. Zhai, H.C. Tao, S.L. Li, ZIF-67-derived FeCoNi-LDH with a 3D nanoflower hierarchical structure for highly efficient oxidation of 5-Hydroxymethylfurfural and coupling seawater splitting hydrogen production, Chemical Engineering Journal 481 (2024) 148429, https://doi.org/10.1016/j.cej.2023.148429.

[10] Y.X. Feng, H.X. Guo, R.L. Smith, Jr., X.H. Qi, Electrocatalytic oxidation of 5-hydroxymethylfurfural to 2,5-furandicarboxylic acid via metal-organic framework-structured hierarchical Co_3O_4 nanoplate arrays, Journal of Colloid and Interface Science 632 (2023) 87-94, https://doi.org/10.1016/j.jcis.2022.11.068.